Coating and stability of thin liquid films on chemically patterned surfaces

B.J. Brasjen and A.A. Darhuber[1]

Mesoscopic Transport Phenomena Group
Department of Applied Physics, Eindhoven University of Technology
P.O. Box 513, 5600 MB Eindhoven, The Netherlands

Presented at the 15th International Coating Science and Technology Symposium,
September 13-15, 2010, St. Paul, MN[2]

Introduction

Many applications in organic electronics require precise liquid film deposition on chemically patterned surfaces. Two strategies for selective deposition onto patterned substrates are 1) applying the liquid exclusively to the desired regions [1,2] and 2) coating the entire surface with a uniform film and relying on subsequent liquid redistribution [3]. In the latter process, it is necessary that this redistribution is completed before the applied solution dries and that no residual volume is left outside the desired regions.

The spontaneous redistribution of a thin liquid film on a chemically homogeneous surface is driven by Van der Waals forces [4-8], which can be represented by a disjoining pressure term [9]. Ruckenstein and Jain showed [6] that films thinner than $O(10^{-8}\,\mathrm{m})$ break up due to long-range molecular forces, whereas films thicker than $h_{eq} = 2\ell_C \sin\theta/2 \sim O(10^{-5} - 10^{-3}\,\mathrm{m})$ are absolutely stable [10]. Films of intermediate thickness are metastable. More recent studies have considered the effect of chemical patterning of the surface, which corresponds to a heterogeneous surface energy [11].

The manufacturing of organic electronic devices employs chemically defined surface patterns that constitute a heterogeneous wettability distribution. As the liquid is usually a solution of active material in a volatile solvent, redistribution takes place simultaneously with evaporative drying of the film, it is desirable that this redistribution is completed before the applied solution dries under the additional condition that, ideally, no residual volume is left outside the wettable patterns. As a first step towards the characterization of the process window, we conducted one-dimensional numerical simulations for pure, non-volatile fluids. We determined the critical film thickness above which no redistribution occurs, the film rupture time, and the residual volume as a function of the surface energy pattern.

Simulation method

In a long-wave (i.e. small slope) approximation, the time evolution of the film thickness h on a chemically patterned substrate is given by the well-known lubrication equation [8]

$$\frac{\partial h}{\partial t} - \nabla_{\parallel}\left(\frac{h^3}{3\mu}\nabla_{\parallel} p\right) = 0, \quad p = \rho g h - \gamma \nabla_{\parallel}^{\,2} h - \Pi, \tag{1}$$

in which p represents the pressure; the fluid properties viscosity, density and surface tension are denoted by μ, ρ and γ respectively. In the case of an evaporating solution, these properties may be concentration dependent. Schwartz and Eley [9] presented a phenomenological model for the disjoining pressure Π, composed of an attractive and a repulsive contribution, given by

$$\Pi = \frac{\gamma(1-\cos\theta_e)}{h^*}\frac{(n-1)(m-1)}{(n-m)}\left(\left(\frac{h^*}{h}\right)^n - \left(\frac{h^*}{h}\right)^m\right) \tag{2}$$

in which n, m and h^* are model parameters and $\theta_e(x,y)$ is the equilibrium contact angle pattern, composed of two types of regions with either the hydrophobic contact angle θ_o or the hydrophilic contact angle θ_i.

---

[1] Author to whom correspondence should be addressed; email: a.a.darhuber@tue.nl, web: www.phys.tue.nl/MTP.

[2] Unpublished. ISCST shall not be responsible for statements or opinions contained in papers or printed in its publications.

The set of eqs. (1,2) is solved using the commercial finite element (FE) software COMSOL 3.5a and MATLAB 7.9.0. We considered periodic contact angle patterns (see e.g. Fig. 1), such that the simulation can be restricted to half a period. In the case of long and straight wettable areas, it suffices to consider a one-dimensional model of half a one-dimensional period of the contact angle pattern (cf. Fig. 1) using symmetry boundary conditions. The initial condition corresponded to a film of uniform thickness $h\ (x,t = 0) = h_0$. The FE discretization is tailored to the contact angle pattern, using smaller mesh elements on the hydrophobic domain (typically 500 nm) and near the hydrophilic/-phobic boundary (typically 1 μm) where the redistribution usually commences; the typical element size on the remainder of the hydrophilic domain was 5 μm.

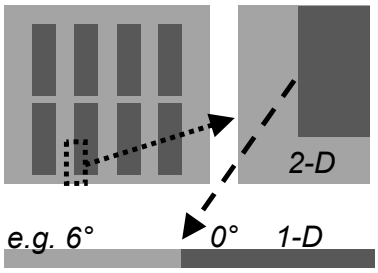

Figure 1: Derivation of model domain from original process substrate.

Since in experiments, the hydrophilic contact angle is usually very small compared to the hydrophobic contact angle, we set it to zero, which allows for coarser FE discretization on the hydrophilic domain and thereby faster computations. A side effect of the zero hydrophilic contact angle is the pinning of the contact line to the hydrophilic/-phobic boundary, which for a non-zero contact angle is not guaranteed. However, any depinning of the contact line can only occur after the dry-spot nucleation and can therefore not modify the presented results.

Results and discussion

Figure 2 shows film thickness profiles $h\ (x,t)$ for different values of the initial thickness h_0 on a heterogeneous substrate with contact angles of $\theta_o = 6°$ and $\theta_i = 0°$, as indicated by the orange and the blue lines, respectively.

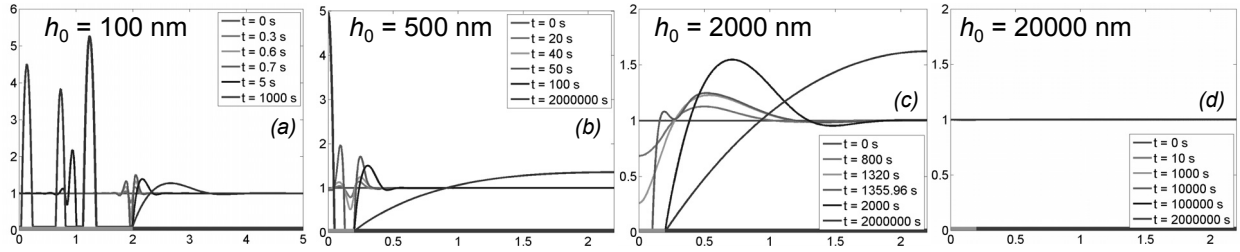

Figure 2: Dewetting on a w_o = 0.4 mm, w_i = 4 mm hydrophobic-hydrophilic substrate; the used values for the liquid properties were μ = 58.3 mPas, γ = 44.0 mN/m and ρ = 1126 kg/m^{-3}.

From the figures, it can clearly be seen that in very thin films [Fig. 2(a)], a dry spot is nucleated close to the hydrophilic/-phobic boundary, from which the dewetting front propagating leftwards over the hydrophobic domain will nucleate more dry spots because Van der Waals forces are dominant in the range of this film thickness. This leads to the formation of a series of droplets that are essentially immobilized and remain on the hydrophobic region. Films of intermediate thickness [Fig. 2(b,c)] nucleate further from the boundary, leading to the formation of a single droplet [Fig. 2(b)] or to complete clearing of the hydrophobic domain [Fig. 2(c)], which is the desired final state. For very thick films, surface tension effects will become dominant over the destabilizing forces and no dry spot is nucleated within experimentally relevant time.

The spontaneous nucleation time τ_s, defined as the time needed for the initially uniform film to nucleate a dry spot, depends on initial film thickness h_0 and hydrophobic contact angle θ_o, as illustrated in Fig. 3. The nucleation time decreases with increasing contact angle and increases with increasing initial thickness. The dependence

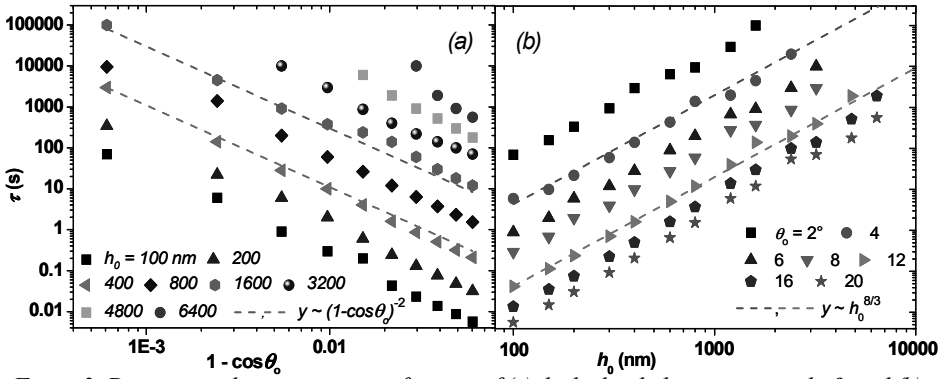

Figure 3: Dry-spot nucleation times as a function of (a) the hydrophobic contact angle θ_o and (b) the initial film thickness h_0.

of τ on θ_o and h_0 can be approximated by a power-law behavior, with exponents close to -2 and +8/3 (dashed lines in Fig. 3), respectively.

Figure 4 shows the residual volume on the hydrophobic part of the substrate, as a function of initial thickness and contact angle. Three different configurations are considered: metastable films that do not break up; unstable films that leave no liquid on the hydrophobic substrate; and unstable films that leave one or more droplets.

From the balance of disjoining pressure and capillary pressure, the transitions are found to satisfy $h \sim (1 - \cos \theta_o)^{1/(m+1)}$, as indicated by the black lines. The stability map of Fig. 4 shows excellent agreement with this dependency.

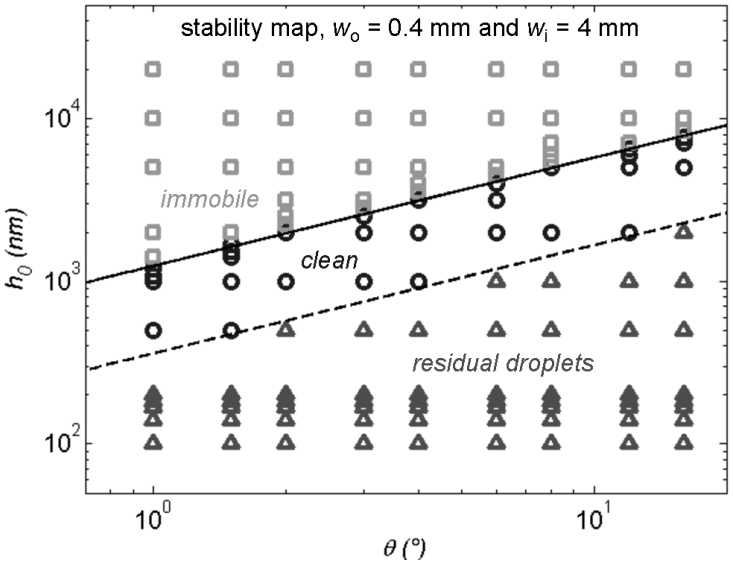

Figure 4: Stability map of thin films on various heterogeneous substrates.

The thickness range between the solid and the dashed black lines in Fig. 4 indicates the desired window of clean operation for the special case of $w_o = 0.4$ mm and $w_i = 4$ mm, which for volatile solutions is further restricted by the drying time condition, with the help of Fig. 3. The resulting parameter window provides a valuable tool in the design of the solution based OLED manufacturing process, providing guidelines for the chemical pattern as well as the coating thickness. Future studies will include the influence of pattern dimensions, evaporation and substrate topology.

References

[1] A. A. Darhuber, S. M. Troian, J. M. Davis, S. M. Miller and S. Wagner, *J. Appl. Phys.* **88**, 5119 (2000).

[2] B.J. Brasjen, A.W. van Cuijk and A.A. Darhuber, *Chem.Eng.Process.,* submitted.

[3] C.L. Bower, E.A. Simister, E. Bonnist, K. Paul, N. Pightling and T.D. Blake, *AIChE J.* **53**, 1644 (2007).

[4] A. Vrij, *Discuss. Faraday Soc.* **42**, 33 (1966).

[5] A. Sheludko, *Adv. Colloid. Interface. Sci*. **1**, 391 (1967).

[6] E. Ruckenstein and R.K. Jain, *J. Chem. Soc,. Faraday Trans.***270**, 132 (1974).

[7] J.P. Burelbach, S.G. Bankoff and S.H. Davis, *J. Fluid Mech.* **195**, 463 (1988).

[8] A. Oron, S.H. Davis and S.G. Bankoff, *Rev. Mod. Phys.* **69**, 931 (1997).

[9] L.W. Schwartz and R.R. Eley, *J. Colloid Interface Sci.* **202**, 173 (1998).

[10] R. Finn, *Equilibrium Capillary Surfaces,* Springer Verlag, New York (1986).

[11] K. Kargupta and A. Sharma, *Langmuir* **18**, 1893 (2002); *Langmuir* **19**, 5153 (2003).